Drug Development and Industrial Pharmacy, 2010; 36(9): 1106–1114

informa
healthcare

ORIGINAL ARTICLE

A pH-sensitive nanocomposite microsphere based on chitosan and montmorillonite with in vitro reduction of the burst release effect

Shuibo Hua[1,2], Huixia Yang[1,2] and Aiqin Wang[1]

[1]*Center of Eco-material and Green Chemistry, Lanzhou Institute of Chemical Physics, Chinese Academy of Sciences, Lanzhou, PR China and* [2]*Graduate University of the Chinese Academy of Sciences, Beijing, PR China*

Abstract

Objective: The aim of this study was to prepare pH-sensitive ofloxacin (OFL)/montmorillonite (MMT)/chitosan (CTS) nanocomposite microspheres that improve the burst release effect of the drug by the solution intercalation technique and emulsification cross-linking techniques. *Methods*: First, OFL/MMT hybrids were prepared through the solution intercalation technique. Then, OFL/MMT-intercalated OFL/MMT/CTS nanocomposite microspheres were obtained through emulsification cross-linking technology. The intercalated nanocomposite was confirmed by Fourier-transform infrared spectroscopy and X-ray diffraction. Finally, in vitro release of OFL from the microspheres was performed in simulated gastric fluids and simulated intestinal fluids. The effect of MMT content on drug encapsulation efficiency and the drug release of the nanocomposite microspheres were investigated. *Results*: The results showed that the release rate of OFL from the nanocomposite microspheres at pH 7.4 was higher than that at pH 1.2. Compared with pure CTS microspheres, the incorporation of certain amount of MMT in the nanocomposite microspheres can enhance the drug encapsulation efficiency and reduce the burst release. *Conclusion*: A sustained release particulate system can be obtained by incorporating MMT into the nanocomposite microspheres and can improve the burst release effect of the drug.

Key words: *Chitosan; drug release; montmorillonite; nanocomposite; ofloxacin*

Introduction

Chitosan (CTS) is derived from the alkaline deacetylation of chitin, which is one of the most abundant polysaccharides in nature. Because of its favorable properties such as enzymatic biodegradability, nontoxicity, and biocompatibility[1], CTS has received considerable attention as a novel drug delivery carrier and has been included in the European *Pharmacopoeia* since 2002. CTS and its derivatives have been proposed as matrices in numerous pharmaceutical formulations, in the form of troche[2], films[3], emulsions[4], transmucosal devices[5], microspheres[6], and so on, for the prolonged release of drugs, delivery of vaccines[7], DNA, insulin[8], and anticancer agents such as 5-fluorouracil[9].

Microsphere is one of the most promising forms as drug delivery system because it can be easily injected or administrated orally into body easily, oriented to the target organ, prolong the half-life, and improve the bioavailability of the encapsulated drug[10]. CTS microspheres loaded with water-soluble drug when brought in contact with acidic media tend to release the active agent quite fast and thereby resulting in a burst effect. Initial burst effect is a common phenomenon with CTS-based delivery systems when loaded with water-soluble drug, and hence, their utility for the controlled delivery of drugs in gastrointestinal tract is questionable. To overcome such initial burst problems, considerable attempts have been made to improve the preparation method of CTS microspheres by coating or grafting with other polymers[11,12]. However, the polymer/clay

Address for correspondence: Prof. Aiqin Wang, Center of Eco-material and Green Chemistry, Lanzhou Institute of Chemical Physics, Chinese Academy of Sciences, Lanzhou 730000, PR China. Tel: +86 931 4968118, Fax: +86 931 8277088. E-mail: aqwang@lzb.ac.cn

(Received 6 Dec 2009; accepted 3 Feb 2010)

ISSN 0363-9045 print/ISSN 1520-5762 online
DOI: 10.3109/03639041003677798

nanocomposite microspheres are rarely used as drug carriers, although they show extraordinary and versatile properties because of the nanometric scale on which the nanoclay particles, with their plate-like shape, would alter the physical and chemical properties of the polymeric materials and improve their mechanical properties and thermal stability[13].

In recent years, based on their high retention capacities as well as swelling and colloidal properties, clays have been proposed as effective materials for modulating drug delivery[14]. Montmorillonite (MMT) is a bioinert clay mineral with fine grain and large interlayer-planar spacing in the (001) plane. It has a superior capability to intercalate large molecules into this space. MMT exhibits good adsorbability, cation-exchange capacity, standout adhesive ability, and drug-carrying capability[15]. Because of these advantages in biomedical applications, it has taken the credit to be called medical clay. A lot of documents reported that the incorporation of organic drug ions in the interlayer space by ion-exchange mechanism[16–18], the so-called intercalation phenomena, was used for the synthesis of drugs/inorganic hybrid materials as molecular capsules. The idea is to store the drug in the interlayer region of the lamellar host and allow the drug release as a consequence of diffusion and/or deintercalation process. However, the amount of intercalated drug is low and the release rate of drug is too quick, because drug is intercalated by ion-exchange process[19].

From these points of view, a combination of MMT with CTS microspheres as a drug carrier is quite attractive and, to the best of our knowledge, there is still no related report. In this study, ofloxacin (OFL, Figure 1), the fluoroquinolone antibiotic, commonly used for the treatment of prophylaxis of a variety of bacterial diseases, was tested as a model cationic drug in the in vitro experiments. First, OFL/MMT hybrids are prepared through the solution intercalation technique; the structure was evaluated by Fourier-transform infrared (FTIR) and X-ray diffraction (XRD). Then, without filtering out the free drug, OFL/MMT-intercalated OFL/MMT/CTS nanocomposite microspheres were obtained through emulsification cross-linking technology. Finally, in vitro release of OFL from the microspheres was performed in simulated gastric fluids (SGF, pH 1.2) and simulated intestinal fluid (SIF) [phosphate buffer solutions (PBS), pH 7.4), and the release profiles were also analyzed by using zero-order, first-order, and Higuchi equation to characterize the drug release mechanism.

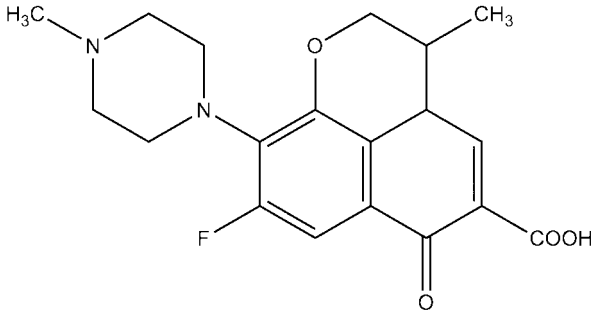

Figure 1. Chemical structure of OFL.

Materials and methods

Materials

CTS (degree of deacetylation, 85%; weight average molecular weight, 9×10^5) from shrimp shell was purchased from Yuhuan Ocean Biochemical Co., Taizhou, China. OFL was obtained from Kunshan Double-crane Pharmaceutical Co. Ltd., Suzhou, China. MMT (99%) was purchased by Zhejiang Sanding Technology Co. Ltd., Shaoxing, China, and was passed through a 320-mesh screen. Glutaraldehyde (GA) 50% (w/w) solution in water, liquid paraffin, and Tween-80 were purchased from Sinopharm Chemical Reagent Co. Ltd., Shanghai, China. SGF (pH 1.2) containing 21.25 mL HCl, 11.18 g KCl in 3000 mL distilled water, and SIF (PBS, pH 7.4), containing 20.4 g K_2HPO_4 and 4.8 g NaOH in 3000 mL distilled water were prepared as described in *US Pharmacopoeia 30*. All other chemicals were of analytical grade and used as received.

Preparation of OFL/MMT hybrids with different soaking time

OFL (0.05 g) and MMT powder (0.10 g) were mixed with 10 mL of 2% (v/v) acetic acid aqueous solution (pH 3.2) in a 50-mL centrifuge tube concomitant with magnetic stirring at room temperature for 0.5, 1, 2, 4, 8, and 24 h, respectively. Then the mixture was centrifuged at $3395 \times g$ for 30 minutes. The supernatant was filtrated through a 0.45-μm membrane filter to remove the floating small MMT particles. The clear supernatant solution was analyzed by HPLC. The mixture after filtration was freeze-dried (–50°C, 24 hours; Alpha 1–2 LD plus, Ger) and ground with mortar and pestle to obtain fine powder for further characterization of FTIR and XRD. The experiment determined how long MMT should be soaked in OFL solution to reach a maximum intercalation.

HPLC (Waters™ 600 Pump, 2998 Photodiode Array Detector) was used to determine the content of OFL using the C18 column. The mixture of acetonitrile and the buffer solutions (25:75, v/v) was used as the mobile phase and OFL was detected at the wavelength of 294 nm. The buffer solution containing 4.0 g ammonium

acetate and 7.0 g sodium perchlorate in 1300 mL water adjusted with phosphoric acid to a pH 2.2 was prepared according to USP 30. Drug content was determined based on the standard curve of OFL, which was achieved from OFL solutions in PBS of pH 7.4 with concentration between 0.002 and 0.01 g/L.

Preparation of OFL/MMT/CTS nanocomposite microspheres

Microspheres were prepared by emulsification chemical cross-linking technique, modified from previous methods[20]. Suitable amount of MMT (0.05, 0.10, and 0.15 g) was dispersed in 10 mL of a 2% (w/w) acetic acid solution, then 0.05 g OFL was added into the suspension, and the mixture was stirred at room temperature for 1 hour (1 hour was enough for the adsorption equilibrium of OFL). CTS (0.2 g) was dissolved directly into the OFL/MMT mixture solution to a final concentration of 2% (w/v) and stirred for 0.5 hour to homogeneity. The mixture was then emulsified into liquid paraffin (20 mL) containing 1% (w/v) Span 80 under mechanical stirring (500 rpm) at room temperature. The system was maintained under agitation for 15 minutes to allow complete emulsification. Thereafter, the formation of the OFL/MMT/CTS microspheres in the oily suspension medium was achieved by the addition of GA solution in water (1.24 g, 5% w/w). Finally after a prefixed cross-linking time of 2.5 hours at 60°C, the yellow power was isolated by centrifugation and washed by heptane two times and three times with petroleum ether and then dried in an oven at 70°C.

Similar procedures were used to prepare pure CTS microspheres without addition of MMT (MS0). Two placebo microspheres with different content of MMT without adding the OFL were also prepared (MS0C and MS2C). The nanocomposite microspheres with various amounts of MMT were termed as MS1–MS3. The code and feed composition of all prepared samples are shown in Table 1.

Determination of EE

The drug encapsulation efficiency (EE) was measured after the extraction from the prepared microspheres. Fifty milligrams of drug-loaded samples was dissolved in 100 mL PBS (pH 7.4) and sonicated for 10 minutes to ensure the complete extraction of OFL from the microspheres. The mixture was stirred magnetically at 1000 rpm for 4 hours and then made up to 250 mL volume with PBS, pH 7.4. After centrifuging at $3395 \times g$ for 30 minutes, these solutions were diluted and subjected to analysis by HPLC. The drug EE and OFL content are expressed as follows:

$$\text{Encapsulation efficiency (\%)} = \frac{\text{practical drug loading}}{\text{theoretical drug loading}} \times 100 \quad (1)$$

$$\text{OFL content (\%)} = \frac{\text{practical drug loading}}{\text{weight of microspheres}} \times 100. \quad (2)$$

Table 1. Feed composition, EE, and drug content of the prepared samples.

Code	CTS	OFL	MMT	EE (%)	OFL content (%)
MS0	0.2	0.05	0	32.71 ± 0.64	6.96 ± 0.34
MS1	0.2	0.05	0.05	63.49 ± 0.54	10.56 ± 0.81
MS2	0.2	0.05	0.10	61.71 ± 0.87	9.56 ± 0.72
MS3	0.2	0.05	0.15	56.46 ± 0.58	6.98 ± 0.44
MS0C	0.2	0	0	—	—
MS2C	0.2	0	0.1	—	—

In vitro drug release experiment

The in vitro drug release tests were carried out using the USP 30 No. 2 dissolution test apparatus (ZRS-8G, Tianjin University Wireless factory, China) fixed with six rotating paddles. Dialysis bags (dialysis tubing, MWCO of 14,000 Da) containing the suspension of microspheres (50 mg) in 5 mL of SGF (pH 1.2) or in PBS (pH 7.4) were placed in 500 mL of the same release medium at 37°C and stirred at 50 rpm. Aliquots of the solutions were collected at the scheduled intervals and filtered with 0.45-μm-pore nylon filters. After each sample collection, the equal amount of fresh release medium at the same temperature was added back. The amount of drug released was monitored by a UV–VIS spectrophotometer (SPECORD 200, Analytik Jera AG) at 294 nm. The UV standard absorbance curve for OFL was established in each release medium. In the concentration range ($2.5–12.5 \times 10^{-5}$ mol/L) investigated, the UV absorbance obeyed the Beer's law.

Characterization

FTIR spectra were recorded on a FTIR spectrophotometer (Thermo Nicolet, NEXUS, TM, USA) in the range of 4000–400 cm^{-1} using KBr pellets. Surface morphology was visualized by scanning electron microscopy (JSM-5600LV, JEOL, Tokyo, Japan) after coating the sample with gold film using an accelerating voltage of 20 kV and by field emission scanning electron microscopy (JSM-6701F). Powder XRD analyses were performed using a diffractometer with Cu anode (PAN alytical X'pert PRO), running at 40 kV and 30 mA, scanning from 3° to 40° at 3°C/min.

Statistical analysis

All the tests including the measurement of drug content determination and in vitro drug cumulative release studies were carried out in triplicate and the average values were reported. Statistical data analysis was performed using the Student's *t*-test with $P < 0.05$ as the minimal level of significance.

Results and discussion

Preparation of OFL/MMT hybrids and OFL/MMT/CTS nanocomposite microspheres

To prepare the OFL/MMT-intercalated OFL/MMT/CTS nanocomposite microspheres, we first prepared the OFL/MMT hybrids. Different technological procedures have been reported for obtaining drug–clay interaction products. Commonly, clay particles are dispersed in the aqueous solution of drug, the dispersions are allowed to equilibrate for a suitable time, and finally solid phases are recovered and dried. The pH value, temperature, and soaking time have great effect on the intercalation capacity[21]. CTS is insoluble at neutral and alkaline solution[22], so the intercalation process in our study was in 2% (v/v) acetic acid solution. The effect of soaking time on the intercalation process of OFL into MMT was studied at room temperature for finding the optimum time of reaching a maximum intercalation. It can be seen from Figure 2 that intercalation of OFL in MMT reached a constant value of about 25% after soaking for 0.5 hour. This fast process was just the same as the report about the intercalation of 5-FU into the MMT[21]. They considered the major mechanisms of intercalation into the adsorption of 5-FU on the free surface of MMT and the replacement of Na^+. The adsorption may occur on the external surfaces and the interlayer spaces of MMT. In the weakly acidic aqueous medium, OFL molecules will be positively charged because of the existence of tertiary amino groups in their molecular structure (Figure 1). As a result, the complementary noncovalent forces formed between the positively charged OFL and the negatively charged surface of MMT platelets. When the concentration gradient of OFL was equal inside and outside of MMT, the diffusion would stop after soaking for a period of time.

To reduce the soaking time and avoid the incomplete intercalation, we selected 1 hour as the optimum soaking time in the subsequent experiments of microsphere preparation.

FTIR spectra

The FTIR spectra of OFL, MMT, and OFL/MMT hybrid are shown in Figure 3. The absorption band at 3623 cm^{-1} is ascribed to the stretching vibration of the interlayer –OH group in MMT and the absorption band at 1714 cm^{-1} belongs to the characteristic absorption of the C=O of OFL, but in the spectrum of the OFL/MMT hybrid, both of them weakened. Besides, the characteristic absorption bands of OFL shifted from 1524 and 1468 cm^{-1} to 1533 and 1474 cm^{-1}, respectively, as a result of intermolecular interaction between OFL and MMT. The result indicates that electrostatic interaction between positively charged OFL and negatively charged MMT has taken place.

FTIR spectral data were also used to confirm the chemical stability of OFL and intercalation of MMT in nanocomposite microsphere, as shown in Figure 4. In case of pure CTS, the characteristic absorption bands at 1651 and 1602 cm^{-1} are assigned to the amide I and $-NH_2$ of CTS, respectively. However, after cross-linking CTS with GA, $-NH_2$ vibration has shifted to 1567 cm^{-1} because of the formation of imine group (MS0C)[23]. When drug is incorporated into the cross-linked microspheres

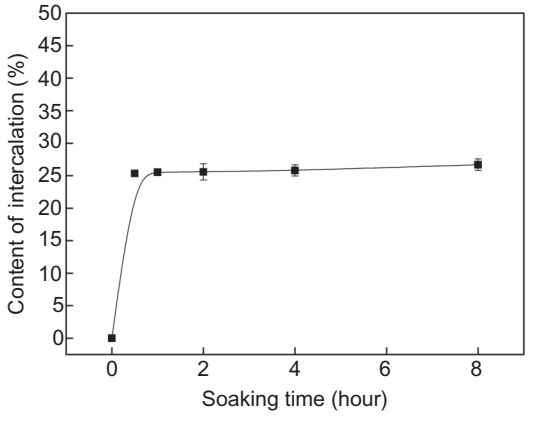

Figure 2. Intercalation of OFL at different soaking times.

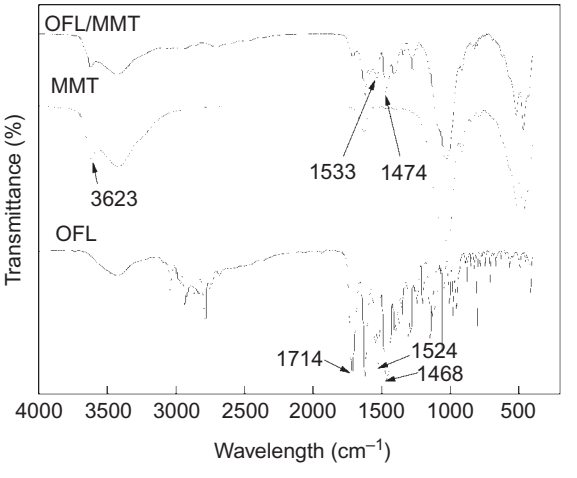

Figure 3. FTIR spectra of OFL, MMT, and OFL/MMT hybrid.

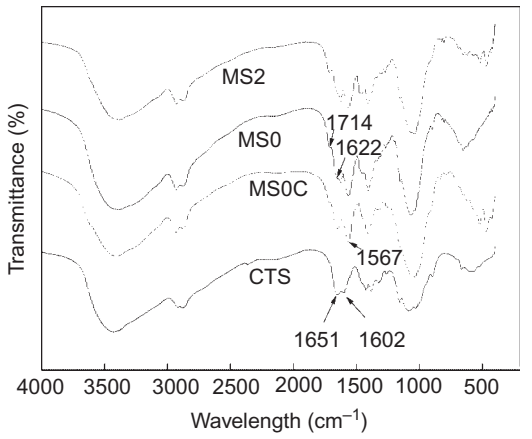

Figure 4. FTIR spectra of CTS, MS0C, MS0, and MS2.

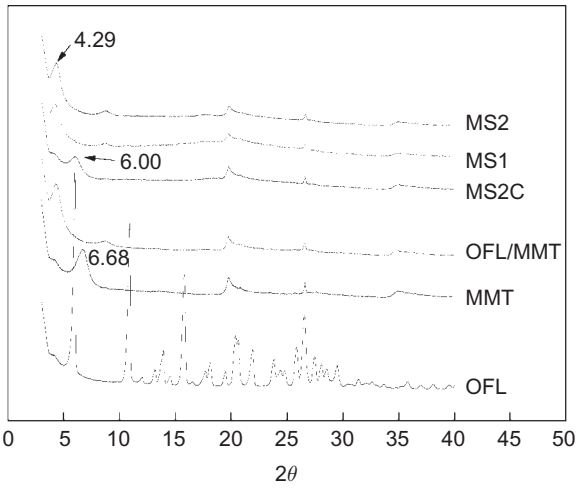

Figure 5. XRD pattern of OFL, MMT, OFL/MMT, MS0C, MS1, and MS2.

(MS0), along with all characteristic absorption bands of MS0C, additional bands at 1714 and 1622 cm^{-1} appeared because of the presence of OFL in the matrix. All these characteristic bands were also clearly observed in the spectrum of MMT-containing nanocomposite microspheres (MS2), indicating that OFL molecules were well entrapped in the microspheres without any chemical deterioration of functional groups (this result also supported by HPLC determination of EE, picture not shown). The absorption band at 3623 cm^{-1} of MMT disappears in the spectrum of the nanocomposite microspheres (MS2), suggesting that the intercalation of OFL molecules into MMT is similar to that of OFL/MMT. FTIR analysis indicates that CTS has been cross-linked with GA and OFL has been encapsulated in the nanocomposite microspheres or stabilized in the interlayers of MMT.

XRD

XRD was a useful tool to test the penetration and possible orientation of cationic drugs in the interlayer space of MMT, by revealing changes in the basal spacing of clay minerals. Figure 5 illustrates the XRD patterns of MMT, OFL, OFL/MMT hybrid, MS1, MS2, and MS2C. OFL has shown characteristic intense peaks of 6° and 10.9° because of the presence of OFL crystals. However, these peaks were not observed in OFL/MMT hybrid and OFL/MMT/CTS nanocomposite microspheres (CMS1–2). This indicates that drug was dispersed at the molecular level in the polymer matrix and in the interlayer of MMT as previously reported with other various organic-nanoclay hybrid systems[3,18], and hence, no crystals were found in the drug-loaded matrices. The XRD pattern of MMT shows a reflection peak at about 6.68°, corresponding to a basal spacing (d) of 1.32 nm. XRD peaks of all the silicates shift to lower angle after forming nanocomposite with OFL (OFL/MMT, MS1, and MS2); the 001 peak of MMT moves from 6.68° to 4.29° (d = 2.07 nm). The 0.74 nm increase of the interlayer distance indicated that OFL molecules were intercalated into the interlayers of MMT and then an intercalated nanostructure was formed. All characteristic crystalline peaks (18° < 2θ <40°) of MMT were seen in the XRD patterns for the hybrid and MMT-containing nanocomposite microspheres prepared in this study.

Hydrophilic OFL contains quaternized amino cations; its chains are more flexible because of the weak intermolecular and intramolecular hydrogen bonds in the aqueous solution, and thereby it can easily exchange with the Na^+ ions of the interlayer and then intercalate into the MMT interlayer, in contrast to analogous polysaccharides (CTS) with coiled or helicoidal structures that are only adsorbed in the external surface of clays or lead to a very small intercalation of MMT (from 6.68° to 6.00° in MS2C). This result was in agreement with a previous study that CTS molecules did not enter sufficiently into the layers of clay structures[24]. These clearly show that in our study the intercalation process was because of the presence of OFL moleculars, but not the CTS macromoleculars.

SEM

It can be seen from Figure 6 that most of the OFL-loaded CTS microspheres were spherical in shape with a smooth surface. MS0 disperse uniformly and the sizes are around 1–15 μm, whereas the surfaces of MMT-containing nanocomposite microspheres (MS1–2) were correspondingly coarse than MS0. This fact reveals that the addition of MMT has an impact on the formation of

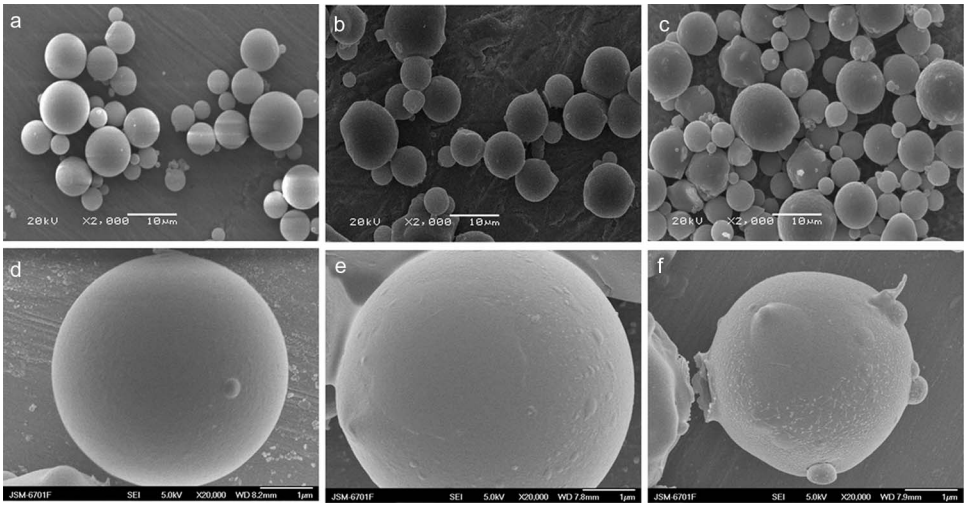

Figure 6. SEM (a–c) and FE-SEM images of the OFL-loaded microspheres of MS0 (a, d), MS1 (b, e), and MS2 (c, f).

nanocomposite microspheres. This change of surface morphology by introducing MMT may influence the swelling ability of corresponding nanocomposite microspheres, and then may have some influences on the release of OFL from the nanocomposite microspheres.

Encapsulation efficiency

Table 1 shows the influence of MMT content on EE of OFL in samples prepared under different conditions. As evident from Table 1, the EE of the microspheres is dependent on the MMT content, which increased with the addition of MMT. This significant difference can be best explained as follows. MMT with large specific area possesses good adsorption capacity, and so it can adsorb OFL well. In the case of certain MMT content, the interaction between OFL and MMT has taken place, which forms more networks to load the drug. However, when the MMT content is too high, the collapse of the polymeric network structure may be induced so that the nanocomposite microspheres cannot load enough OFL. Therefore, MS1 shows the highest drug-loading capacity, followed by MS2, MS3, and MS0.

In vitro release studies

The different types of the nanocomposite microspheres in terms of composition were compared with respect to the release of OFL. The cumulative percentage of OFL released from the microsphere formulations was plotted as a function of time (Figures 7 and 8). The incorporation of MMT into the nanocomposite microspheres brought about a marked reduction in the extent of drug released from the matrix after 4 hours of dissolution ($P < 0.05$).

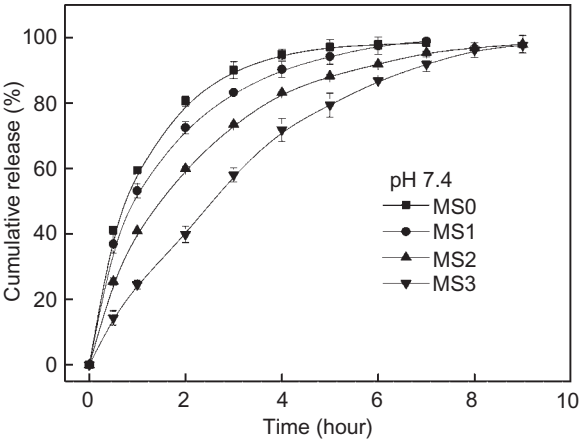

Figure 7. Effect of MMT content on the release profile of the prepared samples at pH 7.4.

The percent of drug released at pH 1.2 was faster than that at pH 7.4 for MS0, which was because of the higher solubility of OFL in acidic medium[25]. However, for MMT-containing nanocomposite microspheres, the percent of drug released at pH 1.2 was slower in comparison to that at pH 7.4 exhibiting pH sensitivity of the nanocomposite microspheres. At the end of 4 hours, 50% of drug load was depleted from MS3 in SGF, in comparison to 71% in PBS (pH 7.4).

The release of OFL from the MMT-containing microspheres at pH 1.2 follows a biphasic pattern, characterized by an initial rapid release period (burst release), followed by a period of slower release. The first rapid release stage was derived from the release of OFL cations from the polymeric matrix of CTS and those adsorbed in the external part of the layer structure of MMT, whereas the second slower release was due to the

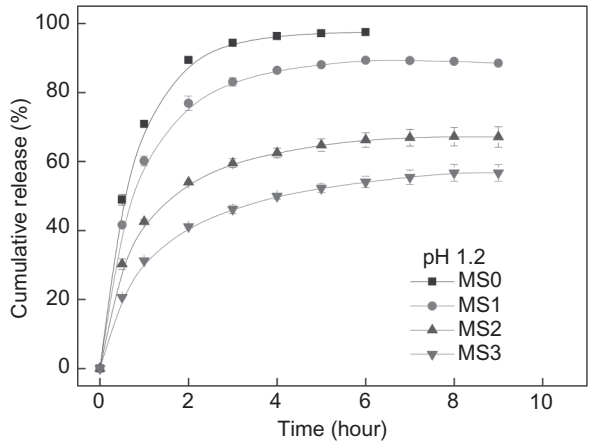

Figure 8. Effect of MMT content on the release profile of the prepared samples at pH 1.2.

exchange of drug ions which are in the internal part of the layers and have to diffuse through the polymeric matrix. This fact was more significant in the release profile of MS3 at pH 1.2, where the release percentage stayed below 60%. This fact may be explained by the existence of electrostatic interactions between the protonated amino groups of OFL cations and the anionic groups from the layers of MMT. Based on the above analyses, the addition of a certain amount of MMT not only improved the drug EE of the nanocomposite microspheres but also provided a slower and continuous drug release.

From these results of characterization, EE and in vitro release studies, a possible scheme for the nanocomposite microsphere is shown in Figure 9. Unlike the ordinary CTS microsphere without addition of MMT (MS0), part of OFL molecules stored in the interlayer of MMT, which lead to a higher EE and a slower drug release behavior.

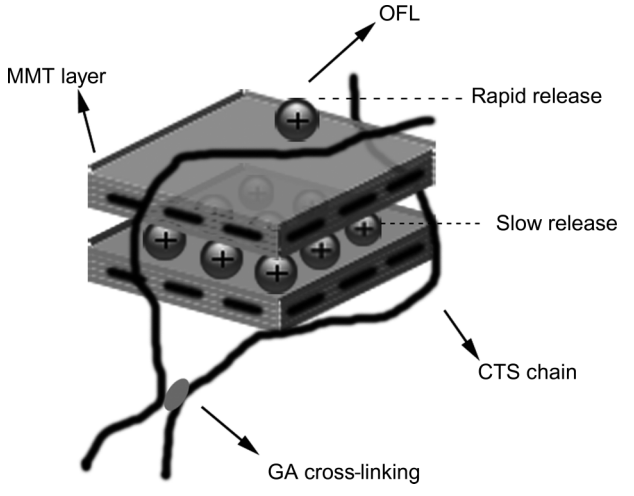

Figure 9. Schematic illustration of the OFL/MMT/CTS nanocomposite microsphere.

Release kinetics

In vitro release data were fitted to various equations to analyze the kinetics and mechanism of drug release from the nanocomposite microspheres. For elucidating kinetics of drug release, the data were analyzed using zero-order equation Equation (3), first-order equation Equation (4)[26,27], and Higuchi's square root model Equation (5)[28]. Where Q is the fraction of drug released in time 't', K is the release constant of respective equations, and t is the release time of the first 4 hours.

$$Q = Kt \tag{3}$$

$$Q = 1 - e^{-Kt} \tag{4}$$

$$Q = K\sqrt{t}. \tag{5}$$

The correlation coefficient (R^2) for Equation (4) was between 0.9888 and 0.9974 for the microspheres released at pH 7.4 (Table 2). This was higher than other kinetic equations, indicating that drug release followed first-order kinetics. The profile released at pH 1.2 showed higher regression coefficient for Higuchi's square root equation, which suggested a time-dependent release mechanism. The observed deviation from Fickian mechanism could be possibly due to higher molecular weight of OFL (361.4), the polymer characteristics (solubility, pK_a, and tortuosity), and the intercalation of MMT[29]. K values showed that, as expected, the release rate decreases with increasing MMT content in the nanocomposite microspheres. The fast initial release rate has been observed in other related studies and explained by the authors as part of the drug being adsorbed outside the nanocomposite microspheres[30]. After the burst release period, the release rate fell as the dominant release mechanism was changed to drug diffusion through the microsphere matrix. The gradual release of OFL in MMT-containing nanocomposite microspheres is due to the exchange of OFL which are in the internal part of the lamellae and have to diffuse through the nanocomposite microspheres (Figure 9). The release half times t_{50} (time required for releasing 50 wt.% of drug) increased with the increase of MMT content, which clearly indicated that a sustained-release particulate system can be obtained by incorporating MMT into the nanocomposite microspheres system. Further studies are needed to evaluate the performance of these systems in vivo and to optimize the formulation.

Table 2. Kinetics analysis of release from the nanocomposite microspheres.

Sample code and pH of release media	Release models and release parameters							
	Zero order		First order			Higuchi		
	K	R^2	K	R^2	t_{50}	K	R^2	t_{50}
MS0, 7.4	0.2905	0.8109	0.7679	0.9954	0.90	0.5222	0.9747	/
MS1, 7.4	0.2737	0.8460	0.6043	0.9926	1.15	0.4827	0.9878	/
MS2, 7.4	0.2403	0.9227	0.4504	0.9974	1.54	0.4167	0.9968	/
MS3, 7.4	0.1894	0.9904	0.2993	0.9888	2.32	0.3193	0.9580	/
MS0, 1.2	0.3116	0.7147	0.9233	0.9662	/	0.5601	0.9287	0.80
MS1, 1.2	0.2743	0.7531	0.5766	0.9325	/	0.4906	0.9494	1.04
MS2, 1.2	0.1965	0.7660	0.2951	0.8691	/	0.3509	0.9570	2.03
MS3, 1.2	0.1528	0.8236	0.2042	0.8908	/	0.2704	0.9795	3.42

Conclusion

In this study, a novel OFL/MMT/CTS nanocomposite microsphere was successfully prepared. OFL was stable in the matrices developed without undergoing any chemical changes during the microsphere production. The nanocomposite microspheres exhibited higher drug-loaded capacity and better drug-controlled release properties in the case of certain MMT incorporation. The drug release rate of the nanocomposite microspheres are influenced by pH of external medium. At pH 1.2, the drug cumulative release ratio of OFL from the nanocomposite microspheres is slower than that at pH 7.4 and decreased with the increase of MMT content. Analysis of the release profiles showed that the drug release predominately followed first-order kinetics and Higuchi's square root equation for releasing at pH 7.4 and pH 1.2, respectively. The decrease of K values and increase of t_{50} with the introduction of MMT clearly indicated that a sustained-release particulate system can be obtained by utilizing MMT into the nanocomposite microspheres system.

Acknowledgment

The authors thank the Western Action Project of CAS (No.KGCX2-YW-501) and the Special Research Fund of Scholarship of Dean of CAS for financial support of this research.

Declaration of interest

The authors report no conflicts of interest. The authors alone are responsible for the content and writing of this paper.

References

1. Muzzarelli R, Baldassarre V, Conti F, Ferrara P, Biagini G, Gazzanelli G, et al. (1988). Biological activity of chitosan ultrastructural study. Biomaterials, 9(3):247–52.
2. Cao J, Sun J, Wang X, Li X, Deng Y. (2009). *N*-Trimethyl chitosan-coated multivesicular liposomes for oxymatrine oral delivery. Drug Dev Ind Pharm, 35(11):1339–47.
3. Depan D, Kumar AP, Singh RP. (2009). Cell proliferation and controlled drug release studies of nanohybrids based on chitosan-*g*-lactic acid and montmorillonite. Acta Biomater, 5:93–100.
4. Lee MK, Chun SK, Choi WJ, Kim JK, Choi SH, Kim A, et al. (2005). The use of chitosan as a condensing agent to enhance emulsion-mediated gene transfer. Biomaterials, 26(14): 2147–56.
5. Jain AK, Chalasani KB, Khar RK, Ahmed FJ, Diwan PV. (2007). Muco-adhesive multivesicular liposomes as an effective carrier for transmucosal insulin delivery. J Drug Target, 15(6): 417–27.
6. Malaekeh-Nikouei B, Tabassi SAS, Jaafari MR. (2008). Preparation, characterization, and mucoadhesive properties of chitosan-coated microspheres encapsulated with cyclosporine A. Drug Dev Ind Pharm, 34(5):492–8.
7. Zhou XF, Zhang XH, Yu XH, Kong W, Shen JC. (2008). The effect of conjugation to gold nanoparticles on the ability of low molecular weight chitosan to transfer DNA vaccine. Biomaterials, 29(1):111–7.
8. Ubaidulla U, Khar RK, Ahmed FJ, Panda AK. (2007). Development and in-vivo evaluation of insulin-loaded chitosan phthalate microspheres for oral delivery. J Pharm Pharmacol, 59(10):1345–51.
9. Akbuga J, Bergisadi N. (1996). 5-fluorouracil-loaded chitosan microspheres: Preparation and release characteristics. J Microencapsul, 13(2):161–68.
10. Kawaguchi H. (2000). Functional polymer microspheres. Prog Polym Sci, 25(8):1171–210.
11. Kumbar SG, Aminabhavi TM. (2003). Synthesis and Characterization of modified chitosan microspheres: Effect of the grafting ratio on the controlled release of nifedipine through microspheres. J Appl Polym Sci, 89:2940–9.
12. Quan JS, Jiang HL, Kim EM, Jeong HJ, Choi YJ, Guo DD, et al. (2008). pH-sensitive and mucoadhesive thiolated Eudragit-coated chitosan microspheres. Int J Pharm, 359(1–2):205–10.
13. Paul DR, Robeson LM. (2008). Polymer nanotechnology: Nanocomposites. Polymer, 49(15):3187–204.
14. Wang XY, Du YM, Yang JH, Tang YF, Luo JW. (2008). Preparation, characterization, and antimicrobial activity of quaternized chitosan/organic montmorillonite nanocomposites. J Biomed Mater Res A, 84A(2):384–90.
15. Aguzzi C, Cerezo P, Viseras C, Caramella C. (2007). Use of clays as drug delivery systems: Possibilities and limitations. Appl Clay Sci, 36(1–3):22–36.
16. Feje'r I, Kate M. (2001). Release of cationic drugs from loaded clay minerals. Colloid Polym Sci, 279:1177–82.
17. Park JK, Bin Choy Y, Oh JM, Kim JY, Hwang SJ, Choy JH. (2008). Controlled release of donepezil intercalated in smectite clays. Int J Pharm, 359(1–2):198–204.
18. Zheng JP, Luan L, Wang HY, Xi LF, Yao KD. (2007). Study on ibuprofen/montmorillonite intercalation composites as drug release system. Appl Clay Sci, 36:297–301.

19. Nunes CD, Vaz PD, Fernandes AC, Ferreira P, Romao CC, Calhorda MJ. (2007). Loading and delivery of sertraline using inorganic micro and mesoporous materials. Eur J Pharm Biopharm, 66(3):357–65.
20. Peng XH, Zhang L. (2005). Surface fabrication of hollow microspheres from N-methylated chitosan cross-linked with glutaraldehyde. Langmuir, 21(3):1091–5.
21. Lin FH, Lee YH, Jian CH, Wong JM, Shieh MJ, Wang, CY. (2002). A study of purified montmorillonite intercalated with 5-fluorouracil as drug carrier. Biomaterials, 23(9):1981–7.
22. Illum L. (1998). Chitosan and its use as a pharmaceutical excipient. Pharm Res, 15(9):1326–31.
23. Kumbar SG, Kulkarni AR, Aminabhavi TM. (2002). Crosslinked chitosan microspheres for encapsulation of diclofenac sodium: effect of crosslinking agent. J Microencapsul, 19(2):173–80.
24. Günister E, Pestreli D, ünlu CH, Atici O, Güngör N. (2007). Synthesis and characterization of chitosan-MMT biocomposite systems. Carbohydr Polym, 67:358–65.
25. Cui Y, Zhang Y, Tang X. (2008). In vitro and in vivo evaluation of ofloxacin sustained release pellets. Int J Pharm, 360(1–2):47–52.
26. Gibaldi M, Feldman S. (1967). Establishment of sink conditions in dissolution rate determinations-theoretical considerations and application to nondisintegrating dosage forms. J Pharm Sci, 56(10):1238–42.
27. Wagner JG. (1969). Interpretation of percent dissolved-time plots derived from *in vitro* testing of conventional tablets and capsules. J Pharm Sci, 58(10):1253–7.
28. Higuchi T. (1963). Mechanism of Sustained-action medication—Theoretical analysis of rate of release of solid drugs dispersed in solid matrices. J Pharm Sci, 52(12):1145–9.
29. Reza MS, Quadir MA, Haider SS. (2003). Comparative evaluation of plastic, hydrophobic and hydrophilic polymers as matrices for controlled-release drug delivery. J Pharm Pharmaceut Sci, 6(2):282–91.
30. Agnihotri SA, Aminabhavi TM. (2004). Controlled release of clozapine through chitosan microparticles prepared by a novel method. J Control Release, 96(2):245–59.